

Plasmon-polariton distributed-feedback laser pumped by a fast drift current in grapheneIgor O. Zolotovskii,^{1,2} Yuliya S. Dadoenkova,¹ Sergey G. Moiseev,^{1,3,4,*} Aleksei S. Kadochkin,^{1,2,5}
Vyacheslav V. Svetukhin,^{1,2} and Andrei A. Fotiadi^{1,6}¹*Ulyanovsk State University, 42 Leo Tolstoy Street, 432017 Ulyanovsk, Russian Federation*²*Institute of Nanotechnologies of Microelectronics of the Russian Academy of Sciences,
32A Leninskiy Prospekt, 119991 Moscow, Russian Federation*³*Kotelnikov Institute of Radio Engineering and Electronics of the Russian Academy of Sciences,
Ulyanovsk Branch, 48/2 Goncharov Street, 432011 Ulyanovsk, Russian Federation*⁴*Ulyanovsk State Technical University, 32 Severny Venetz Street, 432027 Ulyanovsk, Russian Federation*⁵*ITMO University, 49 Kronverkskiy Prospekt, 197101 St. Petersburg, Russian Federation*⁶*Université de Mons, 20 Place du Parc, B7000 Mons, Belgium*

(Received 22 December 2017; published 21 May 2018)

We propose a model of a slow surface plasmon-polariton distributed-feedback laser with pump by drift current. The amplification in the dielectric–semiconducting film–dielectric waveguide structure is created by fast drift current in the graphene layer, placed at the semiconductor/dielectric interface. The feedback is provided due to a periodic change in the thickness of the semiconducting film. We have shown that in such a system it is possible to achieve surface plasmon-polariton generation in the terahertz region.

DOI: [10.1103/PhysRevA.97.053828](https://doi.org/10.1103/PhysRevA.97.053828)**I. INTRODUCTION**

The development of plasmonics over the last two decades opens the possibilities of creating unique devices with parameters significantly exceeding the existing analogs [1–5]. The main advantage of plasmon devices in comparison with classical optical devices is stipulated by the unique properties of surface plasmon polaritons (SPPs)—transverse magnetic polarized optical surface waves which propagate along metal-dielectric or semiconductor-dielectric interfaces and whose fields are coupled to charge density oscillations in the media. SPPs show strong electromagnetic field enhancement, sub-wavelength localization, and high sensitivity to the bounding dielectric environment.

Numerous theoretical and experimental works have been devoted to the study of methods of SPP excitation. To mention a few recent examples, amplitude- and phase-controlled excitation of SPPs with metasurfaces and metastructures consisting of periodic nanoantennas has been demonstrated experimentally in Refs. [6,7]; a nanoantenna for electrical generation of SPPs has been proposed in Ref. [8]; generation of SPP with a microdisk-based plasmonic source [9] and right-angled trapezoid metallic nanoslit [10] have been also discussed.

Amplification with realizable feedback can lead to the generation of SPPs. Such structures, called “spasers” or SPP lasers [11–15], can be used for numerous practical applications [16,17]. At present the problem of effective SPP amplification in active nanostructures is among the main tasks of plasmon technology development [18–21]. Amplification of SPPs can be achieved using the mechanism of energy transfer from plasma oscillations, which are sustained by direct current,

to SSPs, which have an electromagnetic nature [22–27]. A mechanism of the SPP wave amplification due to the energy transfer from an electric drift current wave in graphene into a far-infrared surface wave propagating along a semiconductor-dielectric boundary has been proposed in our paper [28]. It has been shown that in the spectral region of high slowing down of SPP the amplification coefficient can reach values exceeding the SPP damping coefficient. Graphene structures have a record mobility of charge carriers ($1.5 \times 10^4 - 1.5 \times 10^6 \text{ cm}^2 \text{ V}^{-1} \text{ s}^{-1}$ —the maximal mobility of electrons among all known materials [29–31]) which makes graphene plasmonics a promising alternative for use in a variety of applications, in particular, as the future basis of nanoelectronics and on-chip high-speed communication [32,33]. In this paper, we propose a model of plasmon-polariton distributed-feedback laser with pump by fast drift currents in graphene. We show that the peculiarity of such lasers is SPP generation at different frequencies.

II. AMPLIFICATION OF SURFACE PLASMON-POLARITON WAVE BY DRIFT CURRENT PUMP

Let us consider a waveguide structure composed of a semiconducting film with dielectric permittivity in the far-infrared regime $\varepsilon_2 \approx \varepsilon_\infty [1 - \omega_p^2 / \omega(\omega - i\gamma)] = \varepsilon'_2 + i\varepsilon''_2$, $\{\varepsilon'_2, \varepsilon''_2\} < 0$ (with ω and ω_p being the angular and plasma frequencies, respectively, $\gamma > 0$ being a relaxation parameter) and a graphene single layer placed on its interface, as shown in Fig. 1. This bilayer is deposited on a semi-infinite dielectric substrate with dielectric permittivity $\varepsilon_3 > 0$, and the top layer of the waveguide structure is vacuum. We assume that far-infrared SPPs are generating in such a layered thin-film plasmonic waveguide. An electric current is induced by an applied

*serg-moiseev@yandex.ru

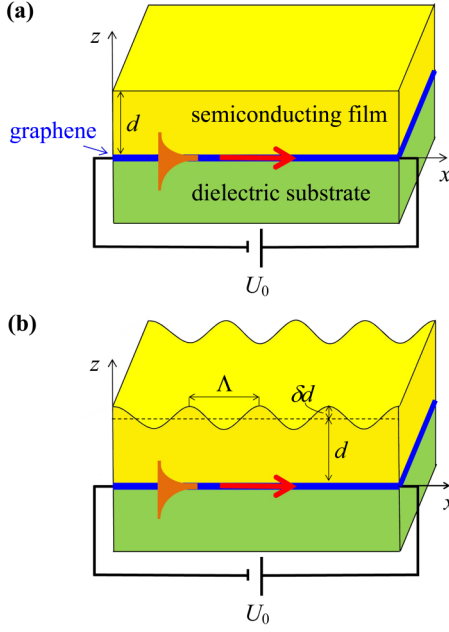


FIG. 1. Schematic of a waveguide structure: a semiconducting film with deposited graphene single layer is placed on a semi-infinite dielectric substrate in the case of the semiconducting film (a) of uniform thickness d ; (b) of spatially modulated thickness with period Λ and modulation depth δd . The direction of the electron flux in the graphene under an applied voltage U_0 is indicated by the red arrow.

voltage U_0 , and the electron flux direction coincides with the SPP propagation direction (the red arrows in Fig. 1). The semiconducting film can be of uniform thickness d [Fig. 1(a)], as well as with spatially modulated thickness with period Λ and small modulation depth δd ($\delta d \ll d$) [Fig. 1(b)]. The spatial modulation of the semiconducting film provides the modification of the SPP propagation constant which is necessary for generation conditions, as will be discussed in detail in Sec. III.

In this section, we perform a brief analysis of the SPP amplification using drift current pumping in the structure schematically illustrated in Fig. 1(a). It is worth noting that in the structure under consideration the drift current is localized in graphene because its conductivity is much higher than that of the semiconducting film [28].

We assume the SPP propagates with the longitudinal component of SPP wave vector $\beta = \beta' + i\beta''$ ($\beta'' < 0$, which corresponds to the SPP damping in the propagation direction) and longitudinal electric field component $\vec{E}_x(x, z, t) = E_x(x, z) \exp[i(\omega t - \beta x)]$. Taking into account the presence of the graphene single layer with the conductivity σ , one can write the relation between the propagation constant and frequency for the SPP wave in this structure in the following form [34].

$$\exp(-2q_2 d) = \frac{q_2 \varepsilon_1 + q_1 \varepsilon_2 q_2 \varepsilon_3 + q_3 \varepsilon_2 + i4\pi q_2 q_3 \sigma / \omega}{q_2 \varepsilon_1 - q_1 \varepsilon_2 q_2 \varepsilon_3 - q_3 \varepsilon_2 + i4\pi q_2 q_3 \sigma / \omega}, \quad (1)$$

where $q_j = \sqrt{\beta^2 - k_0^2 \varepsilon_j}$ is the transverse component of the SPP wave vector in medium $j = 1, 2, 3$ denoting vacuum, semiconducting film, and dielectric substrate, respectively;

$k_0 = \omega/c$ and c are the wave vector and speed of light in vacuum.

Influence of the drift current I on the SPP wave field can be described by the following equation [35,36].

$$\frac{dE_x}{dx} + i \frac{\omega}{V_{\text{ph}}} E_x = -\frac{1}{2} \left(\frac{\omega}{V_{\text{ph}}} \right)^2 K I, \quad (2)$$

where a coupling parameter K can be written as [28]

$$K = \frac{4\pi V_{\text{ph}}^2}{\varepsilon_\infty (\omega^2 + \omega_p^2) V_g L_y h} \eta, \quad (3)$$

with $V_{\text{ph}} = \omega/\beta'$ and $V_g = \partial\omega/\partial\beta'$ being phase and group velocities of the SPP wave, $h = 1/\text{Re}[q_2] \sim 1/\beta'$ being the SPP penetration depth in the semiconducting film, and L_y being the width of the graphene layer. The parameter $\eta = |E_x|^2 / (|E_x|^2 + |E_z|^2)$ is written as [37]

$$\eta \approx \frac{(\varepsilon'_2 k_0)^2}{\beta'^2 (\varepsilon'_2 + \varepsilon_3)^2 + (\varepsilon'_2 k_0)^2}. \quad (4)$$

The SPP wave field modulates the amplitude of the electric current along the graphene layer. To describe the interaction of the current and slow SPP waves, we introduce small perturbations of the current amplitude $\Delta I(x) = I(x) - I_0$ ($\Delta I \ll I_0$), with $I_0 = n_0 |e^*| V_0 L_y$ being an unperturbed current; e^* , n_0 , and V_0 are the effective charge, the surface density, and the drift velocity of charge carriers in graphene, respectively. The evolution of ΔI can be obtained from the following equation [36].

$$\frac{d^2 \Delta I}{dx^2} + 2i \frac{\omega}{V_0} \frac{d \Delta I}{dx} - \frac{1}{V_0^2} (\omega^2 - \omega_q^2) \Delta I = i \frac{\omega}{V_0} \frac{I_0}{2U_0} E_x, \quad (5)$$

where $\omega_q \approx \sqrt{4\pi e^{*2} n_0 \beta' / \varepsilon_\infty m^*}$ is reduced plasma frequency which takes into account the waveguide geometrical parameters, with m_e^* being the effective mass of the charge carriers in graphene.

Thus, mutual influence of the SPP wave field and the drift current leads to the coordinate dependence of their amplitudes. We assume $\{\Delta I(x), E_x(x)\} \sim \exp(-iGx)$, where G is the wave vector of the perturbation. In this case the compatibility condition for the equation set Eqs. (2) and (5) leads to the following dispersion relation:

$$(\omega - G V_{\text{ph}})[(\omega - G V_0)^2 - \omega_q^2] = C^3 \omega^3, \quad (6)$$

where the analog of the Pierce parameter C can be written as [28]

$$C \approx \left(\frac{\eta}{2} \frac{\omega_q^2}{\omega^2 + \omega_p^2} \frac{V_{\text{ph}}}{V_g} \right)^{1/3}. \quad (7)$$

The complex roots of Eq. (6) give the value of the SPP amplification coefficient α as

$$\alpha = |\text{Im}(G)|. \quad (8)$$

III. GENERATION OF SURFACE PLASMON POLARITONS IN STRUCTURE WITH DISTRIBUTED FEEDBACK

Let us consider the conditions for the generation of a SPP wave in a structure with distributed feedback provided by continuous scattering of a surface wave from a periodic perturbation of the thickness of a semiconductor film with a spatial period Λ [as shown in Fig. 1(b)]. We consider the case of slightly varying film thickness $\delta d = \chi d$, when the depth of modulation changes within the range $10^{-4} \leq \chi \leq 10^{-2}$.

In the case of a periodically profiled film, forward and backward electromagnetic waves with amplitudes $A \sim \exp[-i\beta'x + (\alpha - |\beta''|)x]$ and $B \sim \exp[i(\beta' - 2\pi m/\Lambda)x + |\beta''|x]$ (m is any integer), respectively, form in this waveguide system. Taking into account wave-vector detuning $\Delta\beta = \beta' - \pi m/\Lambda$, the dynamics of the forward and backward surface waves under the condition of an undepleted pump by the drift current wave is described by a system of equations known from the theory of lasers with distributed feedback [38].

$$\begin{aligned} \frac{dA}{dx} &= (\alpha - |\beta''|)A - i\kappa B \exp(2i\Delta\beta x), \\ \frac{dB}{dx} &= |\beta''|B + i\kappa A \exp(-2i\Delta\beta x), \end{aligned} \quad (9)$$

where the interwave coupling intensity parameter κ can be estimated as

$$\kappa \approx \frac{1}{2}\chi\beta'. \quad (10)$$

In Eq. (9) it is taken into account that a graphene film with a current provides amplification only for the direct wave A , whereas the re-reflected backward wave B is not amplified due to the opposite directions of phase velocity of the backward wave and drift current velocity, which makes the phase matching conditions unsatisfied.

Using an ansatz $A = \tilde{A} \exp[(\alpha - |\beta''|)x]$ and $B = \tilde{B} \exp(|\beta''|x)$, the equation set Eq. (9) can be written as

$$\begin{aligned} \frac{d\tilde{A}}{dx} &= -i\kappa \tilde{B} \exp\{2i[\Delta\beta + ig]x\}, \\ \frac{d\tilde{B}}{dx} &= i\kappa \tilde{A} \exp\{-2i[\Delta\beta + ig]x\}, \end{aligned} \quad (11)$$

where $g = \alpha/2 - |\beta''|$. Taking into account the boundary conditions $A(0) = A_0$ and $B(L) = 0$, the solution of Eq. (11) is written as

$$\begin{aligned} A(x) &= A_0 \frac{(g - i\Delta\beta) \sinh[S(L-x)] - S \cosh[S(L-x)]}{(g - i\Delta\beta) \sinh(SL) - S \cosh(SL)} \\ &\quad \times \exp\left\{\left(i\Delta\beta + \frac{\alpha}{2}\right)x\right\}, \\ B(x) &= A_0 \frac{i\kappa \sinh[S(L-x)]}{(g - i\Delta\beta) \sinh(SL) - S \cosh(SL)} \\ &\quad \times \exp\left\{\left(-i\Delta\beta + \frac{\alpha}{2}\right)x\right\}, \end{aligned} \quad (12)$$

with $S^2 = \kappa^2 + (g - i\Delta\beta)^2$. On the basis of the solutions obtained for the amplitudes of the forward and backward SPP waves, the reflection R and transmission T coefficients take

the form

$$\begin{aligned} R &= \left| \frac{B(0)}{A(0)} \right|^2 = \left| \frac{\kappa \sinh(SL)}{(g - i\Delta\beta) \sinh(SL) - S \cosh(SL)} \right|^2, \\ T &= \left| \frac{A(L)}{A(0)} \right|^2 = \left| \frac{S \exp(\alpha L/2)}{(g - i\Delta\beta) \sinh(SL) - S \cosh(SL)} \right|^2. \end{aligned} \quad (13)$$

$$(14)$$

From Eqs. (13) and (14) it follows that efficiency of the energy transfer between the forward and backward SPP waves depends on the detuning value $\Delta\beta$. By choosing the period Λ of the structure and the length L of the waveguide (length of the graphene layer), it is possible to manage the interaction between the waves.

In the approximation of inexhaustible pumping at certain parameters of the system, the energy of the generated waves can increase indefinitely, i.e., $\{R, T\} \rightarrow \infty$. This condition is fulfilled provided that the denominators of Eqs. (13) and (14) tend to zero, so that the following relation is satisfied:

$$(g - i\Delta\beta) \sinh(SL) = S \cosh(SL). \quad (15)$$

However, from Eq. (14) it follows that in the transmission spectrum $T(\omega, \Lambda)$ for some values of period Λ there are spectral ranges with central frequencies corresponding to the propagation constants $\beta'_m = m\pi/\Lambda$, where the SPP generation does not occur. We will call the corresponding area a ‘‘plasmonic band gap’’ (by analogy with the photonic band gap in photonic crystals). The SPP generation is possible at the plasmonic band-gap edges when the condition Eq. (15) is fulfilled.

IV. RESULTS OF NUMERICAL CALCULATIONS

In this section, we present results of the numerical analysis of the equations presented above, and discuss the regimes of amplification and generation of SPP waves. For the numerical calculations, we took the following values of the material parameters: $\varepsilon_\infty = 10.89$, $\omega_p = 34.2 \times 10^{12} \text{s}^{-1}$ (Ref. [39]), and $\gamma = 0.01 \omega_p$ for semiconductor (GaAs); the dielectric permittivities of the cladding and substrate are $\varepsilon_1 = 1$ (air), $\varepsilon_3 = 4$ (SiO₂), respectively. The thickness of the semiconducting film is $d = 30 \text{ nm}$, and the waveguide length $L = 250 \mu\text{m}$. For dc current in the graphene, the surface charge carrier density is $\Pi_0 \approx 10^{12} \text{cm}^{-2}$ (Ref. [29]). We assume the charges in graphene move with velocity $V_0 = 0.8 \times 10^8 \text{cm/s}$ [40–42].

The graphene surface conductivity in the terahertz regime is calculated using the following expression which takes into account the loss in graphene [43,44].

$$\begin{aligned} \sigma(\omega, \mu_c, \Gamma, T) &= \frac{ie^2(\omega + i2\Gamma)}{\pi \hbar} \left[\int_{-\infty}^{\infty} \frac{f_d(-\omega) - f_d(\omega)}{(\omega + i2\Gamma)^2 - 4\omega^2} d\omega \right. \\ &\quad \left. - \frac{1}{(\omega + i2\Gamma)^2} \int_{-\infty}^{\infty} \frac{\partial f_d(\omega)}{\partial \omega} |\omega| d\omega \right], \end{aligned} \quad (16)$$

where $f_d = \{\exp[(\hbar\omega - \mu_c)/k_B T] + 1\}^{-1}$ is the Fermi-Dirac distribution, μ_c is the chemical potential, T is temperature, Γ is a phenomenological scattering rate, \hbar is the reduced Planck constant, and k_B is the Boltzmann constant. In our calculations, we assume $T = 300 \text{ K}$, $\mu_c = 0.2 \text{ eV}$, and $\Gamma = 1 \text{ meV}$.

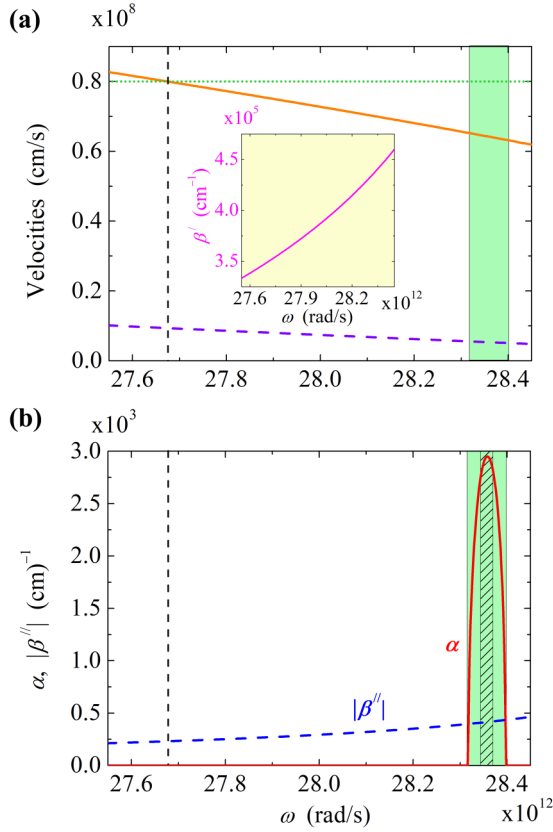


FIG. 2. Frequency dispersion of (a) the SPP phase velocity V_{ph} (solid orange line), group velocity V_g (dashed violet line), and drift current velocity V_0 (dotted green line); (b) amplification coefficient α (solid red line) and absolute value of loss coefficient $|\beta''|$ (dashed blue line) for the parameters given in the text. The inset in (a) shows the dispersion of the SPP propagation constant β' . Dashed vertical line shows frequency corresponding to condition $V_{ph} = V_0$. Green area shows frequency interval when $\alpha > |\beta''|$, and shaded area corresponds to SPP generation regime (see comments to Fig. 3).

First we show the frequency dispersion of the parameters of the SPP in the case of no spatial modulation of the semiconducting film [the structure schematically illustrated in Fig. 1(a)]. Phase and group velocities of SPP are shown in Fig. 2(a) with solid orange and dotted violet lines, respectively, and the dotted green line corresponds to drift current velocity in graphene. The dispersion of the low-frequency branch of the SPP propagation constant β' is illustrated in the inset in Fig. 2(a) in order to show that the values of $\beta' \sim 10^5 \text{ cm}^{-1}$ are two orders of magnitude larger than the values of $k_0 \sim 10^3 \text{ cm}^{-1}$ in the considered frequency range, so $\beta' \gg k_0$. From Fig. 2(a) it follows out that the SPP wave in a semiconducting film can be slowed down to velocities of the same order of magnitude as the drift velocity of the current carriers ($V_{ph} < 10^8 \text{ cm/s}$), which allows the effective transfer of energy from the current carriers to the surface electromagnetic wave. One can see that the condition $V_{ph} = V_0$ is fulfilled at the frequency $\omega_{syn} \approx 27.67 \times 10^{12} \text{ rad/s}$, as shown with the vertical dashed line.

The dispersions of the SPP amplification coefficient α and Ohmic loss coefficient $|\beta''|$ are shown in Fig. 2(b) with solid red

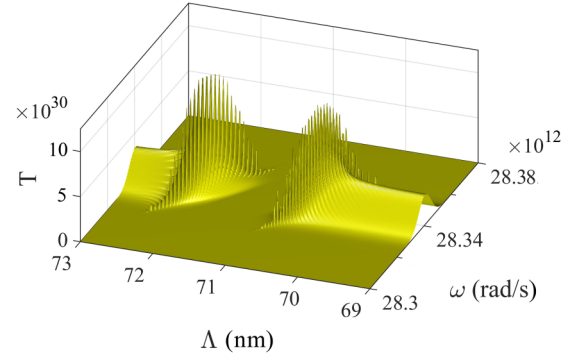


FIG. 3. Evolution of the transmission coefficient T with angular frequency ω of SPP and period of the structure Λ . The parameters of the structure are the same as for Fig. 2.

and dashed blue lines, respectively. As follows from Fig. 2(b), the amplification linewidth is $\Delta\omega_\alpha \approx 0.08 \times 10^{12} \text{ rad/s}$. Comparing the solid red and dashed blue lines, one can see that the total loss compensation ($\alpha > |\beta''|$, green area) takes place almost within the whole amplification line. Note that the maximal amplification coefficient $\alpha_{max} \approx 3 \times 10^3 \text{ cm}^{-1}$ is about six times larger than the loss coefficient $|\beta''|$. It should be noted that amplification in the system occurs at frequencies higher than ω_{syn} , i.e., when $V_{ph} < V_0$, in contrast to our previous paper [28], where in a similar system the maximal amplification took place at ω_{syn} due to neglecting the reduced plasma frequency of graphene. This regime is connected to Cherenkov radiation in the plasmonic waveguide [45]. The corresponding amplification mode of the electromagnetic waves is typical, in general, for microwave amplifiers and generators (traveling and backward wave tubes) [46]. For these devices, the largest amplification also occurs under the conditions when the drift velocity of the current exceeds the value of the phase velocity of the amplified wave.

Further we analyze the behavior of the SPP transmission coefficient in the case of spatially modulated semiconducting film thickness. The transmittivity T calculated using Eq. (14) is shown in Fig. 3 as a function of the angular frequency ω of SPP and period Λ for the modulation depth $\chi = 10^{-2}$ and $m = 1$. The depth of spatial modulation in this case is $\delta d = 1 \text{ nm}$. One can see that within the frequency range $(28.335 - 28.345) \times 10^{12} \text{ rad/s}$ a plasmonic transition band exists, i.e., the frequency interval with high values of transmittivity. Due to high values of the SPP loss coefficient, the generation band ($T \gg 1$) is located inside the amplification line ($\alpha > 0$), and its width is $\Delta\omega_g \approx 10^{10} \text{ rad/s}$ [see shaded area in Fig. 2(b)].

One can see from Fig. 3 that for the modulation period within the range $71 \text{ nm} < \Lambda < 71.5 \text{ nm}$ the plasmonic transition band is interrupted with a plasmonic band gap characterized by extremely low transmittivity ($T \rightarrow 0$). For the structure under consideration the Λ width of the plasmonic band gap is about 1.5 nm. The position of the plasmonic band gap in the Λ axis depends on the frequency of the radiation, namely, the band-gap center corresponds to the modulation period $\Lambda = \pi/\beta'(\omega)$. In the vicinity of the plasmonic band-gap edges the transmittivity demonstrates an abrupt increase with $T \gg 1$, which corresponds to the SPP generation conditions, Eq. (15).

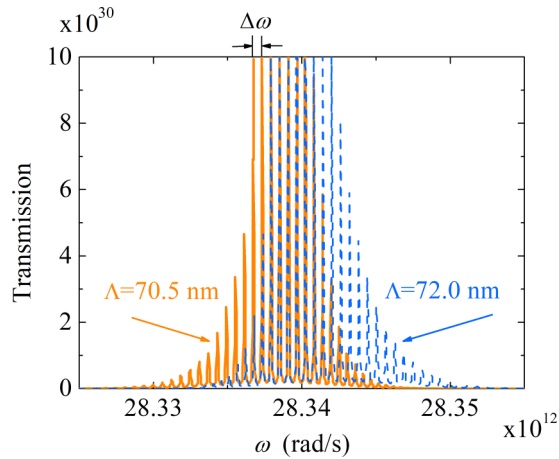


FIG. 4. Cross sections of Fig. 3 at two values of the structure period $\Lambda = 70.5$ nm (solid orange line) and $\Lambda = 72$ nm (dashed blue line).

From Fig. 3 it one can also see that for every modulation period Λ the dependence of the transmittivity T on the radiation frequency represents a group of peaks. The amplitude of these generation peaks is determined by the shape of the amplification line $\alpha(\omega)$ of the SPP. The generation peaks shift from high-frequency band-gap edge to low-frequency edge with increase of Λ . To show in detail the behavior of the transmittivity in the vicinity of the plasmonic band gap, in Fig. 4 we plot cross sections of the T surface at two values of the structure period $L = 70.5$ nm (solid orange line) and $\Lambda = 72$ nm (dashed blue line), which correspond to the opposite edges of the forbidden band gap. One can see that, for each Λ , the SPP generation takes place at several equidistant frequencies around $\omega = 28.34 \times 10^{12}$ rad/s with step $\Delta\omega \approx 6 \times 10^8$ rad/s.

V. CONCLUSIONS

We have shown the possibility of surface plasmon-polariton generation in a waveguiding system containing a graphene

single layer. The proposed model is a kind of hybrid of a distributed-feedback laser and a traveling-wave tube, well known in microwave technology. In this type of plasmon laser (spaser) the amplification is created by fast drift currents propagating in the graphene, and the feedback is realized due to a periodic change in the thickness of the semiconducting film. In such planar structure it is possible to achieve the surface plasmon-polariton generation simultaneously at several frequencies.

The frequency and amplitude of the generated SPP waves can vary due to changes in such structure parameters as the thickness and modulation period of the thickness of the semiconductor film. To keep the SPP generation regime it is necessary to control the feasibility of the synchronism condition for the velocities of the motion of the charge carriers in graphene V_0 and the phase velocity V_{ph} of the SPP wave. Note that an increase of the film thickness leads to an increase of the phase velocity of the SPP, which requires larger drift velocities V_0 . Fabrication of composite graphene structures with large Fermi velocities and, thus, larger V_0 , is currently in progress. Such techniques are called “Fermi velocity engineering” [47,48]. The first experimental results indicate the actual fabrication of structures with the Fermi velocity up to 3×10^8 cm/s [49–51]. Numerical estimations show that for such values of the drift velocity in graphene the generation of SPPs will be possible in a semiconductor film of thickness of about 100 nm.

The proposed model of ultracompact generator of terahertz surface plasmon polaritons with current pumping can find wide application both in communication technologies and in the development of ultrafast optical logic elements.

ACKNOWLEDGMENTS

This work was supported by the Ministry of Education and Science of the Russian Federation (Project No. 14.Z50.31.0015, State Contracts No. 3.7614.2017/9.10, No. 3.5698.2017/9.10, No. 3.3889.2017/4.6, and No. 16.2773.2017/4.6), and the Russian Foundation for Basic Research (Project No. 17-02-01382).

- [1] *Plasmonics: From Basic to Advanced Topics*, Springer Series in Optical Sciences, edited by S. Enoch and N. Bonod (Springer, Berlin, 2012).
- [2] *Active Plasmonics and Tuneable Plasmonic Metamaterials*, edited by A. V Zayats and S. A. Maier (Wiley, New York, 2013).
- [3] A. de Hoogh, A. Opheij, M. Wulf, N. Rotenberg, and L. Kuipers, *ACS Photonics* **3**, 1446 (2016).
- [4] R. Karlsson, *J. Mol. Recognit.* **17**, 151 (2004).
- [5] A. Alù and N. Engheta, in *Metamaterials and Plasmonics: Fundamentals, Modelling, Applications*, edited by S. Zouhdi, A. Sihvola, and A. Vinogradov (Springer, New York, 2009), pp. 37–47.
- [6] H. Mühlenbernd, P. Georgi, N. Pholchai, L. Huang, G. Li, S. Zhang, and T. Zentgraf, *ACS Photonics* **3**, 124 (2016).
- [7] D. Wintz, A. Ambrosio, A. Y. Zhu, P. Genevet, and F. Capasso, *ACS Photonics* **4**, 22 (2017).
- [8] F. Bigourdan, J.-P. Hugonin, F. Marquier, C. Sauvan, and J.-J. Greffet, *Phys. Rev. Lett.* **116**, 106803 (2016).
- [9] O. Kurniawan, I. Ahmed, and E. P. Li, *IEEE Photonics J.* **3**, 344 (2011).
- [10] X. Yang, J. Wang, X. H. Lim, Z. Xu, J. Teng, and D. H. Zhang, *J. Phys. D: Appl. Phys.* **50**, 045101 (2017).
- [11] A. Tredicucci, C. Gmachl, F. Capasso, A. L. Hutchinson, D. L. Sivco, and A. Y. Cho, *Appl. Phys. Lett.* **76**, 2164 (2000).
- [12] A. Babuty, A. Bousseksou, J.-P. Tetienne, I. M. Doyen, C. Sirtori, G. Beaudoin, I. Sagnes, Y. De Wilde, and R. Colombelli, *Phys. Rev. Lett.* **104**, 226806 (2010).
- [13] R. F. Oulton, V. J. Sorger, T. Zentgraf, R. M. Ma, C. Gladden, L. Dai, G. Bartal, and X. Zhang, *Nature* **461**, 629 (2009).
- [14] M. A. Noginov, G. Zhu, M. Mayy, B. A. Ritzo, N. Noginova, and V. A. Podolskiy, *Phys. Rev. Lett.* **101**, 226806 (2008).
- [15] R. Li, A. Banerjee, and H. Grebel, *Opt. Express* **17**, 1622 (2009).

- [16] A. G. Curto, G. Volpe, T. H. Taminiu, M. P. Kreuzer, R. Quidant, and N. F. van Hulst, *Science* **329**, 930 (2010).
- [17] M. S. Tame, K. R. McEnergy, S. K. Özdemir, J. Lee, S. A. Maier, and M. S. Kim, *Nat. Phys.* **9**, 329 (2013).
- [18] P. Hawrylak and J. J. Quinn, *Appl. Phys. Lett.* **49**, 280 (1986).
- [19] K. Kempa, P. Bakshi, and J. Cen, in *Advanced Processing of Semiconductor Devices II*, edited by H. G. Craighead and J. Narayan (SPIE, Bellingham, WA, 1988), pp. 62.
- [20] S. A. Maier, *Opt. Commun.* **258**, 295 (2006).
- [21] M. Hrton, M. A. Poyli, V. M. Silkin, and J. Aizpurua, *Ann. Phys.* **524**, 751 (2012).
- [22] B. G. Martin, J. J. Quinn, and R. F. Wallis, *Surf. Sci.* **105**, 145 (1981).
- [23] R. F. Wallis, B. G. Martin, and J. J. Quinn, *Physica B+C (Amsterdam)* **117–118**, 828 (1983).
- [24] B. G. Martin, A. A. Maradudin, and R. F. Wallis, *Surf. Sci.* **91**, 37 (1980).
- [25] V. Lozovskii, S. Schrader, and A. Tsykhonya, *Opt. Commun.* **282**, 3257 (2009).
- [26] C. M. Aryal, B. Y.-K. Hu, and A.-P. Jauho, *Phys. Rev. B* **94**, 115401 (2016).
- [27] T. A. Morgado and M. G. Silveirinha, *Phys. Rev. Lett.* **119**, 133901 (2017).
- [28] Y. S. Dadoenkova, S. G. Moiseev, A. S. Abramov, A. S. Kadochkin, A. A. Fotiadi, and I. O. Zolotovskii, *Ann. Phys.* **529**, 1700037 (2017).
- [29] K. S. Novoselov, A. K. Geim, S. V. Morozov, D. Jiang, M. I. Katsnelson, I. V. Grigorieva, S. V. Dubonos, and A. A. Firsov, *Nature* **438**, 197 (2005).
- [30] K. S. Novoselov, *Rev. Mod. Phys.* **83**, 837 (2011).
- [31] A. K. Geim, *Rev. Mod. Phys.* **83**, 851 (2011).
- [32] Q. Bao and K. P. Loh, *ACS Nano* **6**, 3677 (2012).
- [33] M. Miscuglio, D. Spirito, R. P. Zaccaria, and R. Krahne, *ACS Photonics* **3**, 2170 (2016).
- [34] P. A. D. Gonçalves and N. M. R. Peres, *An Introduction to Graphene Plasmonics* (World Scientific Publishing Co. Pte. Ltd., Singapore, 2016).
- [35] J. Pierce, *Electrons and Waves* (Anchor Books, New York, 1964).
- [36] D. I. Trubetskov and A. E. Khramov, *Lectures on Microwave Electronics for Physicists* (Fizmatlit, Moscow, 2003).
- [37] D. G. Sannikov, D. I. Sementsov, and S. V. Zhirmov, *Solid State Phenom.* **152–153**, 369 (2009).
- [38] A. Yariv and P. Yeh, *Optical Waves in Crystals* (Wiley, New York, 1984).
- [39] S. Adachi, *Physical Properties of III-V Semiconductor Compounds: InP, InAs, GaAs, GaP, InGaAs, and InGaAsP* (Wiley, New York, 1992).
- [40] M. A. Yamoah, W. Yang, E. Pop, and D. Goldhaber-Gordon, *ACS Nano* **11**, 9914 (2017).
- [41] H. Ramamoorthy, R. Somphonsane, J. Radice, G. He, C. P. Kwan, and J. P. Bird, *Nano Lett.* **16**, 399 (2016).
- [42] M. D. Ozdemir, O. Atasever, B. Ozdemir, Z. Yarar, and M. Ozdemir, *AIP Adv.* **5**, 077101 (2015).
- [43] G. W. Hanson, *J. Appl. Phys.* **103**, 064302 (2008).
- [44] V. P. Gusynin, S. G. Sharapov, and J. P. Carbotte, *J. Phys.: Condens. Matter* **19**, 026222 (2007).
- [45] S. Liu, P. Zhang, W. Liu, S. Gong, R. Zhong, Y. Zhang, and M. Hu, *Phys. Rev. Lett.* **109**, 153902 (2012).
- [46] S. E. Tsimring, *Electron Beams and Microwave Vacuum Electronics* (Wiley, New York, 2006).
- [47] C. Hwang, D. A. Siegel, S. K. Mo, W. Regan, A. Ismach, Y. Zhang, A. Zettl, and A. Lanzara, *Sci. Rep.* **2**, 2 (2012).
- [48] P. V. Ratnikov and A. P. Silin, *JETP Lett.* **100**, 311 (2014).
- [49] D. C. Elias, R. V. Gorbachev, A. S. Mayorov, S. V. Morozov, A. A. Zhukov, P. Blake, L. A. Ponomarenko, I. V. Grigorieva, K. S. Novoselov, F. Guinea, and A. K. Geim, *Nat. Phys.* **7**, 701 (2011).
- [50] Z. Q. Li, E. A. Henriksen, Z. Jiang, Z. Hao, M. C. Martin, P. Kim, H. L. Stormer, and D. N. Basov, *Nat. Phys.* **4**, 532 (2008).
- [51] G. Li, A. Luican, and E. Y. Andrei, *Phys. Rev. Lett.* **102**, 176804 (2009).